

# Three-dimensional neutral particle transport simulation for analyzing polarization resolved H-alpha spectra in the large helical device

M. Shoji<sup>a,\*</sup>, A. Iwamae<sup>b</sup>, M. Goto<sup>a</sup>, A. Sakaue<sup>b</sup>, M. Atake<sup>b</sup>, S. Masuzaki<sup>a</sup>, J. Miyazawa<sup>a</sup>, N. Ohyabu<sup>a</sup>, A. Komori<sup>a</sup>, LHD Experimental Groups<sup>a</sup>

<sup>a</sup> National Institute for Fusion Science, 322-6 Oroshi-cho, Toki 509-5292, Japan

<sup>b</sup> Department of Engineering Physics and Mechanics, Graduate School of Engineering, Kyoto University, Kyoto 606-8501, Japan

---

## Abstract

Change of  $H_{\alpha}$  intensity profiles depending on magnetic configurations is observed in the divertor plasma. It can be explained by the magnetic field line structures in the ergodic layer and the divertor legs. The behavior of neutral particles in the plasma periphery is investigated by a three-dimensional neutral particle transport simulation code which assumes that the distribution of the plasma flow onto the divertor plates corresponds to that of the strike points calculated by magnetic field line traces. Vertical  $H_{\alpha}$  intensity profiles and polarization resolved  $H_{\alpha}$  spectra are calculated by the simulation code including the effect of Doppler broadening, fine structure splitting and polarization of the  $H_{\alpha}$  emission, which agree well with the measurements in various magnetic configurations. It shows spontaneous formation of high neutral density in inboard side of the torus, which is independent of the magnetic configurations in LHD.

© 2007 Elsevier B.V. All rights reserved.

PACS: 52.25.Ya; 52.55.Hc; 52.65.Pp

Keywords: Divertor neutrals; EIRENE; Hydrogen; LHD; Visible imaging

---

## 1. Introduction

Control of the influx of neutral particles from the plasma periphery in the magnetic confinement devices play an important role for achieving the H-mode, the edge thermal transport barrier and long pulse discharges [1,2]. The closed divertor configuration is one of the promising measures to

achieve efficient particle control and reduction of the heat load on divertor plates by divertor detachment. Understanding of the behavior of neutral particles in the plasma periphery is an essential issue for designing the closed divertor.

Study on the closed divertor is one of the urgent tasks for the large helical device (LHD) which is the largest heliotron-type superconducting machine with  $l/m = 2/10$ , where  $l$  and  $m$  are the poloidal and toroidal mode numbers of helical coils, respectively [3]. One of the characteristics of LHD plasmas

---

\* Corresponding author. Fax: +81 572 58 2618.

E-mail address: [shoji@LHD.nifs.ac.jp](mailto:shoji@LHD.nifs.ac.jp) (M. Shoji).

is the existence of an ergodic layer surrounding the last closed flux surface (LCFS) with four divertor legs where the magnetic field lines directly connect to divertor plates with short connection length ( $\sim 2$  m). The position of the magnetic axis ( $R_{ax}$ ) can be changed by controlling poloidal coil currents, which also changes magnetic field line structures in the ergodic layer and the divertor legs.

Neutral particles in the plasma periphery have been measured with  $H_\alpha$  emission detectors and a  $H_\alpha$  filtered CCD camera. Change of the  $H_\alpha$  intensity profile depending on the position of the magnetic axis was observed. The behavior of neutral particles in various magnetic configurations is investigated with a 3-d neutral particle transport simulation code (EIRENE) with newly considering Doppler effect, the fine structure of  $H_\alpha$  line (Zeeman effect) and polarization of the emission, which proposes a promising closed divertor configuration for LHD plasmas.

## 2. $H_\alpha$ intensity profiles and the distribution of the strike points

Fig. 1 shows the experimental setup of diagnostic systems for neutral particle measurement.  $H_\alpha$  inten-

sity profiles have been observed with a tangentially viewing CCD camera ( $H_\alpha$  filtered) located on an outer port (3-O) for monitoring divertor plates and divertor legs near a lower port (2.5-L) [4]. Fig. 1(a) illustrates the pictorial view of the peripheral plasma from the camera position. The intensity profile of  $H_\alpha$  emission has been measured with an absolutely calibrated 10ch vertical detector array at an outer port (1-O), where the cross section of the plasma is horizontally elongated as shown in Fig. 1(b) and (c). The  $H_\alpha$  spectra are measured with polarization separation optics (PSO) which can resolve the spectra into two orthogonally polarized components. The separated lights (e-ray and o-ray) are transmitted to a spectrometer. The location and intensity of the emission along the line of sight are identified by analyzing the spectra by the least-squares fitting [5].

Fig. 2(a) is the images of a  $H_\alpha$  intensity profile in two different magnetic configurations ( $R_{ax} = 3.60$  and  $3.75$  m). The change of the intensity profile depending on the magnetic configurations is observable, showing unbalanced  $H_\alpha$  intensity on the divertor legs. Fig. 2(b) shows the colored contour plots of strike point density on the poloidal and toroidal plane. The strike points are calculated by

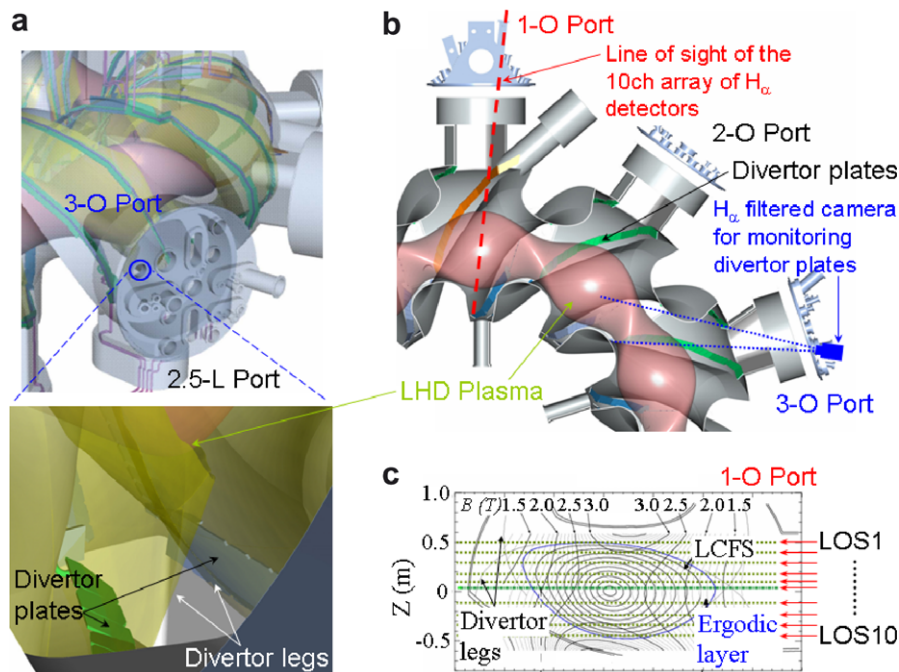


Fig. 1. (a) Bird's eye view of the LHD vacuum vessel with the pictorial view of the divertor region from the camera position, (b) cross-sectional view of the vacuum vessel with diagnostic systems for measuring neutral hydrogen in the plasma periphery, and (c) map of the magnetic surfaces and the magnetic field on the poloidal surface of the line of sight of a  $H_\alpha$  detector array.

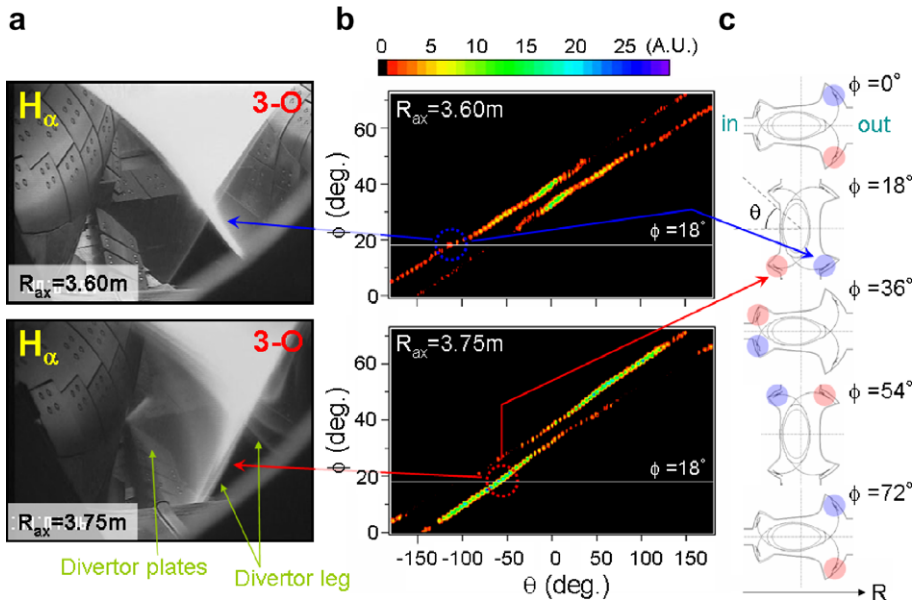


Fig. 2. (a) Observed  $H_\alpha$  intensity profiles in magnetic configurations ( $R_{ax} = 3.60\text{ m}$  and  $3.75\text{ m}$ ), (b) colored contour plots of strike point density on the poloidal and toroidal plane, and (c) poloidal cross-sections of the vacuum vessel at five different toroidal angles. Blue and red circles indicate the position of the strike points of two divertor legs.

magnetic field line traces from the LCFS. The bright divertor leg in the two magnetic configurations corresponds to the leg connecting to outer and inner divertor plates at a toroidal angle of  $\phi = 18^\circ$ , respectively (see Fig. 2(c)). The measured temperature and density of the divertor leg are about  $30\text{ eV}$  and several  $10^{17}\text{ m}^{-3}$ , respectively, which indicates that these plasma parameters are in an ionizing phase for hydrogen neutrals. Thus, the  $H_\alpha$  intensity increases with neutral density on the divertor leg. Near the region where the strike points are concentrated, the neutral density should be high by strong hydrogen recycling due to the plasma flow along the magnetic field lines. Accordingly, change of the intensity profiles can be explained by the distribution of the strike points depending on the magnetic configurations.

### 3. Spatial profiles of neutral density in three magnetic configurations

Three-dimensional profiles of neutral density are calculated by a Monte Carlo neutral particle transport simulation code (EIRENE) [6]. The poloidal and toroidal distribution of the plasma flow onto the divertor plates is assumed to be that of the strike points. This assumption is supported by the  $H_\alpha$  intensity profiles and measurements of divertor

plate temperatures [7]. Fig. 3(a) gives the toroidal distribution of the strike point density in three magnetic configurations ( $R_{ax} = 3.50, 3.65$  and  $3.75\text{ m}$ ). Red solid lines and blue broken lines mean the strike point density at the poloidal positions shown as red and blue circles in Fig. 2(c), respectively. The strike points are distributed around out-board, inboard and upper/lower side of the torus in the three magnetic configurations, respectively. The behavior of the reflected hydrogen atoms from the strike points is determined on the bases of the database calculated by the TRIM code [8]. Non-reflected neutrals are treated as released molecules with the velocity corresponding to the room temperature ( $300\text{ K}$ ).

The cross-sections of the calculated  $H_\alpha$  emission profile on the plane of the line of sight of the detectors are described in Fig. 3(b), which show higher emission at the inboard side in all the magnetic configurations. The emission is calculated by using the measured plasma parameter profiles (the temperature and density in the plasma periphery (ergodic layer) are about  $200\text{ eV}$  and  $0.5\text{--}2.0 \times 10^{19}\text{ m}^{-3}$ , respectively). Red closed circles in Fig. 4(a) are the vertical profile of the  $H_\alpha$  intensity obtained by integrating the calculated emission along the line of sight. The emission is derived by a collisional-radiative model of hydrogen [9]. Green squares indicate

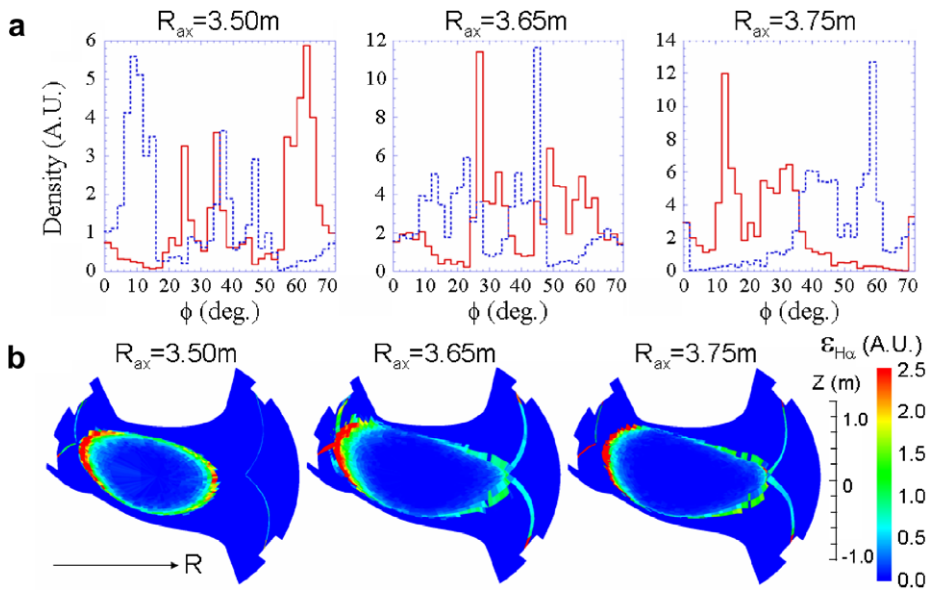


Fig. 3. (a) Toroidal distribution of strike point density in three magnetic configurations ( $R_{ax} = 3.50, 3.65$  and  $3.75$  m), and (b) calculations of the  $H_\alpha$  emission profile on the poloidal plane of the line of sight of the detectors in the three magnetic configurations.

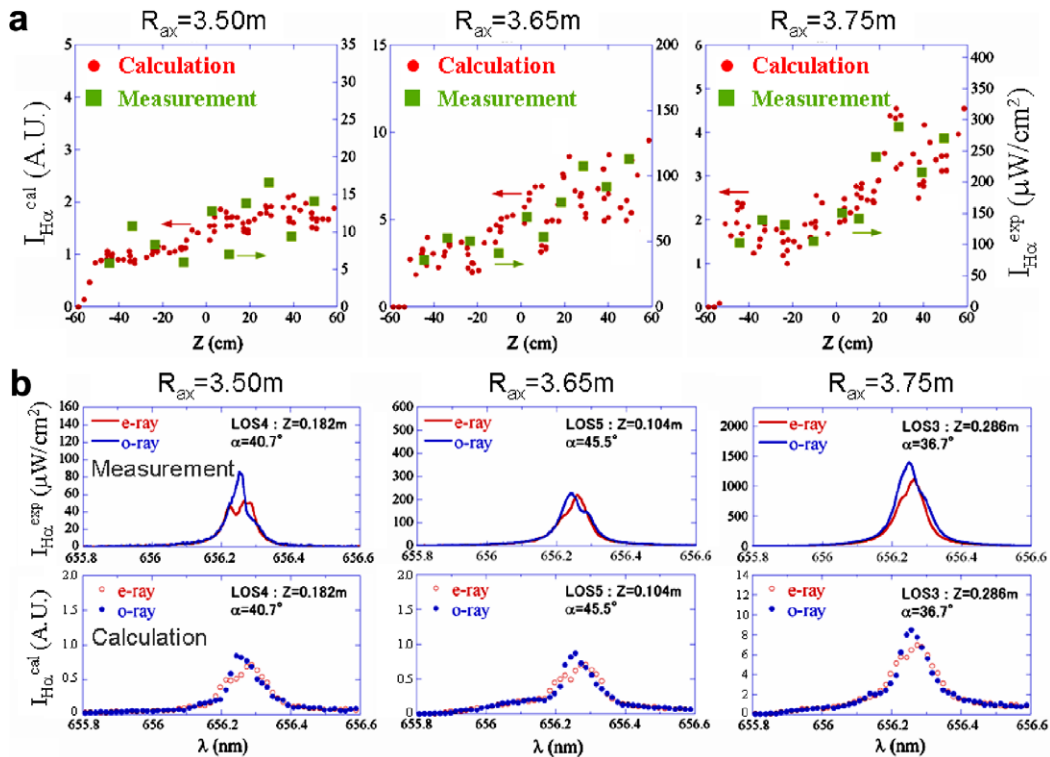


Fig. 4. (a) Vertical  $H_\alpha$  intensity profiles obtained by integrating the calculated emission along the line of sight of the detectors (red circles) and measurements (green squares), and (b) measurements and calculations of the polarization resolved  $H_\alpha$  spectra (e-ray and o-ray) in three magnetic configurations ( $R_{ax} = 3.50, 3.65$  and  $3.75$  m).

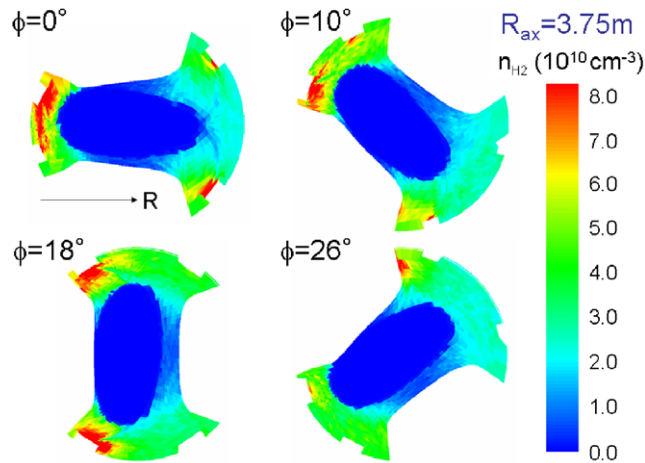


Fig. 5. Poloidal cross-sections of the calculated density profile of neutral hydrogen molecules in a magnetic configuration ( $R_{ax} = 3.75$  m) at four different toroidal angles.

the measured  $H_{\alpha}$  intensity profiles. The calculations quite agree with the measurements in all the magnetic configurations.

Polarization resolved spectra are also measured in these magnetic configurations. The calculations of the spectra (e-ray and o-ray) are derived from the velocity of neutral particles calculated by the neutral transport simulation code with newly considering the following three effects:

1. Doppler broadening due to the velocity of neutral hydrogen [10];
2. fine structure splitting of  $H_{\alpha}$  line spectrum by the Zeeman effect [5];
3. polarization of  $H_{\alpha}$  emission by the effect of the magnetic field.

The instrumental function of the detectors, the magnetic field, and the polarization angle ( $\alpha$ ) of the PSOs are also considered. Fig. 4(b) gives the measurements and calculations of the spectra in the three magnetic configurations, which shows agreement between them within the experimental error (the error of the intensity ratio of the two rays is  $\sim 20\%$ ). The measured narrow peak of the o-ray ( $\lambda \sim 656.24$  nm) for  $R_{ax} = 3.50$  m is likely to be reflected light from the vacuum vessel because of the unbalanced intensity of the two rays [11]. The reason for the slight difference in a short wavelength side of the spectra can be attributed to overestimated backscattered particles predicted by TRIM code which assumes no contaminated layer on the target surface. The neutral transport simulation

can reproduce the measurements of the  $H_{\alpha}$  vertical intensity profile and the polarization resolved spectra, which verify the high neutral density in the inboard side of the torus in spite of the different distribution of the gas source depending on the magnetic configurations (see Fig. 3(a)). The reason for the high neutral density can be explained by the three-dimensionally complicated shape of the vacuum vessel in which the divertor region in the inboard side locates in narrow space between the two helical coils.

Fig. 5 shows the four poloidal cross-sections of the calculated density profile of neutral hydrogen molecules for  $R_{ax} = 3.75$  m, which clearly shows relatively high molecular density ( $\sim 8.0 \times 10^{16} \text{ m}^{-3}$ ) in the inboard side of the torus. The density is consistent with that estimated from the neutral gas pressure measured with a fast ion gauge in this experimental condition ( $n_e \sim 3 \times 10^{19} \text{ m}^{-3}$ , no pellets), which is about one order of magnitude lower than that for efficient particle control. It strongly suggests that the closed divertor configuration in the inboard side is a promising and realistic measure to raise neutral density in the divertor region with keeping the field of view from plasma diagnostics installed in outer ports.

#### 4. Conclusions

Change of the  $H_{\alpha}$  intensity profiles depending on the magnetic configurations can be explained by the magnetic field line structure in the plasma periphery. Three-dimensional neutral density profiles are

calculated by the simulation code on the assumption that the distributions of the plasma flow to the divertor plates correspond to that of the strike points. The simulation code including Doppler broadening, fine structure splitting and polarization of the  $H_{\alpha}$  emission gives the reasonable agreement between the calculations and the measurements (vertical  $H_{\alpha}$  intensity profiles and polarization resolved spectra). It clearly shows formation of high neutral density in inboard side of the torus which is independent of magnetic configurations.

### **Acknowledgement**

The author (M.S.) thank technical officers in NIFS for their experimental support. The simulation was performed by cooperation with NIFS computer and information network center.

### **References**

- [1] N. Ohya, K. Narihara, H. Funaba, et al., *Phys. Rev. Lett.* 84 (2000) 103.
- [2] M. Shoji, R. Kumazawa, K. Saito, et al., *J. Nucl. Mater.* 337–339 (2005) 186.
- [3] O. Motojima, H. Yamada, A. Komori, et al., *Phys. Plasmas* 6 (1999) 1843.
- [4] M. Shoji, T. Watanabe, LHD Experimental Groups, *IEEE Trans. Plasma Sci.* 33 (2) (2005) 440.
- [5] A. Iwamae, M. Hayakawa, M. Atake, et al., *Phys. Plasmas* 12 (2005) 042501.
- [6] D. Reiter, P. Gogen, U. Samm, *J. Nucl. Mater.* 196–198 (1992) 1059.
- [7] S. Masuzaki, T. Morisaki, N. Ohya, et al., *Nucl. Fusion* 42 (2002) 750.
- [8] J.P. Biersack, W. Eckstein, *Appl. Phys.* 34 (1984) 73.
- [9] K. Sawada, T. Fujimoto, *J. Appl. Phys.* 78 (1995) 2913.
- [10] D.P. Stotler, C.H. Skinner, R.V. Budny, et al., *Phys. Plasmas* 3 (11) (1996) 4084.
- [11] M. Goto, S. Morita, *Phys. Rev. E* 65 (2002) 026401.